Nano-Structures & Nano-Objects 19 (2019) 100361

Contents lists available at ScienceDirect

Nano-Structures & Nano-Objects

journal homepage: www.elsevier.com/locate/nanoso

Synthesis of organic phase change materials by using carbon nanotubes as filler material

Suhanyaa S. Magendran [a], Fahad Saleem Ahmed Khan [a], N.M. Mubarak [a,*], Mohammad Khalid [b,*], Rashmi Walvekar [c], E.C. Abdullah [d,*], Sabzoi Nizamuddin [e], Rama Rao Karri [f]

[a] Department of Chemical Engineering, Faculty of Engineering and Science, Curtin University, 98009 Sarawak, Malaysia
[b] Graphene & Advanced 2D Materials Research Group (GAMRG), School of Science and Technology, Sunway University, No. 5, Jalan Universiti, Bandar Sunway, 47500 Subang Jaya, Selangor, Malaysia
[c] School of Engineering, Taylor's University, 47500 Subang Jaya, Selangor, Malaysia
[d] Department of Chemical Process Engineering, Malaysia-Japan International Institute of Technology (MJIIT) Universiti Teknologi Malaysia (UTM), Jalan Sultan Yahya Petra, 54100 Kuala Lumpur, Malaysia
[e] School of Engineering, RMIT University, Melbourne, 3001, Australia
[f] Petroleum & Chemical Engineering, Universiti Teknologi Brunei, Brunei Darussalam

GRAPHICAL ABSTRACT

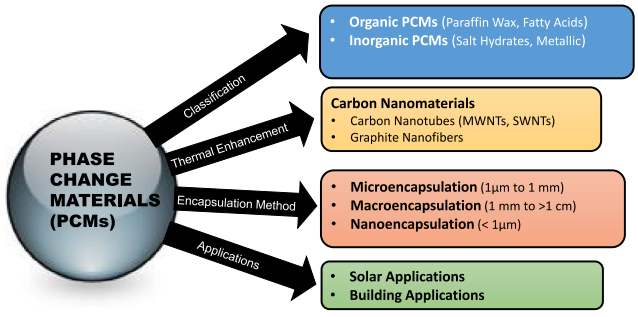

ARTICLE INFO

Article history:
Received 20 December 2018
Received in revised form 16 May 2019
Accepted 2 July 2019

Keywords:
Phase change materials
Organic phase change materials
Carbon nanotubes
Microscopic characterization
Thermal conductivity

ABSTRACT

In the past decade, nanotechnology field has becoming one of the main attraction of many industries due to higher concern on the important of nanotechnology materials. Multi-walled carbon nanotubes (MWCNTs) acts as fillers and impair the development of organic phase change materials (PCMs) based on their microscopic characterization, thermal and mechanical properties. In the present study, various weight percentage of MWCNTs samples were prepared. The parameter involved in these study includes on different weight percentage of MWCNTs and PCM, operating temperature and sonification method. The MWCNTs were characterized by using Field Emission Scanning Electron Microscope (FESEM), thermogravimetric (TGA) analysis, Energy dispersive X-ray (EDX), and Fourier Transform Infrared Spectroscopy (FTIR). Meanwhile, mechanical analysis such as flexural and tensile testing were also carried out under mechanical testing. The optimum conditions used are by dispersing MWCNTs in PCM in the ratio of 1:1 in respective temperature conditions and also via ultra-sonification treatment method at 65 °C for 1.5 h. Synthesis of PCM by using MWCNTs as fillers can result in higher yields with high density of carbon content bond and lower weight loss on the surface of MWCNTs. The results has indicated that the organic PCM can be synthesized by using carbon nanotubes and can be use.

1. Introduction

Continuous ascent of emission caused by greenhouse gas, fuel prices increasing day by day in market, and fossil fuel constrained

* Corresponding authors.
E-mail addresses: mubarak.mujawar@curtin.edu.my, mubarak.yaseen@gmail.com (N.M. Mubarak), khalids@sunway.edu.my (M. Khalid), ezzatc@utm.my, ezzatchan@gmail.com (E.C. Abdullah).

https://doi.org/10.1016/j.nanoso.2019.100361
2352-507X/

accessibility is the main working prospective to use different wellsprings based on sustainable energy. Thermal energy storage or known as TES is the main energy that to be used later relatively into another form meanwhile the two primary kinds of energy storage options are known as sensible heat storage and latent heat storage. The issues of shortage of energy and ecological pollution are the resulting factors from fossil fuel burning are the main reason winding up more crucial currently. Phase transition changes occurs to hold on energy in latent TES system such as cold storage water, ice and melting paraffin wax. During phase changing, PCMs are materials that has the capability to store huge amount of energy while initiating higher TES as an important role. Holding up excessive heating and discharging on the place and time required, compromises in thermal energy storage (TES). This also helps to fill up the gap between demand in thermal energy and supply of each other [1]. PCM has a lower thermal conductivity which leads to preventing faster heat transfer thus, became the barrier of power capacity of these framework [2]. Thermal energy in phase change material (PCM) by collecting and discharging are especially compelling, as these type of material can store higher amount of heat although they have their restricted temperature, based on different constrained volume [3].

PCMs is comprehensively characterized in two different sorts known as organic PCMs and inorganic PCMs. Inorganic PCMs such as salt hydrates, or also known as Glauber's salt, were few of the research that has studied in the early stages for the development of latent TES materials [4]. They were also well-known with their few appealing characteristics such as high thermal conductivity, increase in latent heat values, non-flammable and decrease in cost difference between other organic compounds [5]. Based on this scenario, with their unaccepted attributes has lead the research study to focus more by investigating on the organic PCMs. Organic PCMs are known and widely used for their various qualities which made them even more valuable in components with higher latent heat storage. Their characteristics such as non-corrosive, increase in latent heat, soften consistently, easily recycled, and reveal some and zero supercooling [3] has made them to be better and effective than the inorganic PCMs. In spite of the fact that the initial cost showed better increment than the inorganic PCMs [6], but cost of installation was much ruthless. With their lower thermal conductivity, volume changes during phase change is higher, flammable, and produce dangerous vapour during combustion were few of their significant characteristics that made slight difference than the inorganic type [7]. From that point forward various investigations have concentrated on organic PCMs. With their better thermal stability, freezing without supercooling characteristics, capacity to consistently melt, non-segregation, and toxic-less made to provide better considerable measures based on their favourable circumstances. Paraffin and fatty acids are known as one of the encouraging compare to their other subordinates between organic PCM. Moreover, organic PCM can be grouped into few different sorts, for example, polyalcohol and polyethylene, that experiences solid–solid phase transformation by absorbing and discharging at a fixed temperature of extensive quantity of the latent heat, have been focused as a favourable PCMs [8].

Encapsulation of PCMs, impregnation of PCM into polyurethane (PU) froth, and a balance form by introducing PCM as a cross section of other material are examples of frameworks has been done earlier. The main strategy that has been studied is the encapsulation of PCM. These have been divided into two different principles which is Micro and Macro Encapsulation. Microencapsulation can be compressed as assurance of unstable, sensitive materials from the surroundings, better managing of process by enhancing solubility and dispensability of core and shell materials, time-span by preventing degradative responses and evaporation and, protected and appropriate handling of core materials [7]. Meanwhile, the second containment method is macroencapsulation method, that owing to the advantage like its sensitiveness towards both liquid and air for heat transfer fluid and the demand towards ships and handles were less. Both micro- and macro-encapsulation method can be prepared by using three different types of methods such as physico-mechanical method, chemical properties or physico-chemical method based on organic PCM with physico-chemical applications [9,10]

Among various nanomaterials, carbon nanotubes (CNTs) are generally pictured as a graphene sheet rolled in the form of cylinder. There are two fundamental types of CNTs with high structural flawlessness, known as single-walled CNTs (SWCNTs) and multi-walled CNTs (MWCNTs) [11]. The SWCNTs compromises of a single graphite sheet wrapped into a round and hollow tube meanwhile the MWCNTs includes a variety of concentric cylinders. CNTs does not only work to build thermal conductivity of PCMs, yet it helps to decrease level of cooling under certain temperature and enhance on the PCM's stability range. CNTs demonstrates huge potential with included substances to enhance on better and efficient thermal conductivity for latent heat TES [12]. The carbon nanomaterial such as CNTs, graphene and graphene oxide and nano clay has tremendous application in energy storage, composite, strain sensing and waste water treatment application [13–23]. There were many previous researches that has been carried out by researchers on observe and analysis on the paraffin type of organic phase change for the industrial applications as they consist of characteristics in a betterment in such applications and many other considerations as shown in Table 3. Commercial grade paraffin has been observed and made an analysis on the differences in melting temperature, latent heat and specific heat have also proved that small scale of difference in melting point and latent heat of fusion of paraffin can be observed [24,25]. The phase change materials such as palmitic acid with dispersion of CNTs can enhanced on the thermal conductivity and acts as filler materials [5,26].

Therefore, in this study, paraffin wax containing CNTs is utilized for the synthesis of organic phase change materials in various applications. Comparison of the performance based on paraffin wax, a type of organic PCM, has been performed to highlight on the enforcement of using CNTs as fillers and methods based on different process parameters such as thermal, mechanical and microscopic characterization analysis were investigated and further discussed. Finally, the modifications in synthesizing organic PCM by using CNTs has been carried out and hence novelties were created and discussed to improve on the dispersion of CNTs together with paraffin wax.

2. Materials and method

2.1. Material preparation

In the current work, paraffin wax with melting point of 59 °C were selected and used to represent on the paraffin under the organic phase change materials. Paraffin wax is selected due to its unique characteristics such as it is less hazardous than any other paraffin materials and significantly shows better latent heat compared to any other PCMs. Although paraffin shows higher latent heat of fusion and increase in melting temperature than any other fatty acids, but it has been commercialized in many research projects. The accuracy of the apparatus were verified before and after the measurements [5], MWCNTs was obtained from previous work [27].

Table 1
Mixing formulation of CNTs and organic phase change materials.

Sample code	Paraffin content (wt. %)
MWCNTs – 1 wt.%	1
MWCNTs – 3 wt.%	3
MWCNTs – 5 wt.%	5

2.2. Material preparation

The paraffin wax received are without any chemicals and fully purified raw materials. Firstly, the paraffin wax undergoes pre-melting process and are degassed in a vacuum oven at 105 °C for time period of three hours respectively. The two types of carbon nanotube also undergo the same pre-drying process in the oven under the same condition of paraffin wax. Then, the organic PCM was prepared with a good mixing called as melt-mixing scheme. The CNTs with elevated mass fraction of 1 wt% to 5 wt% are prepared with increase of 2 wt%, respectively as shown in Table 1. The sample preparations then undergo two steps known as dispersion and solidification step. During the first dispersion step, the carbon nanotubes selected is added into the molten paraffin wax with respective mass and then the suspensions with a magnetic stirrer for 15 min were prepared with strong shear mixing. Then, it undergoes with an intensive ultrasonication in a time period of 90 min. Throughout these step, the samples were maintained at temperature at above melting point of the paraffin wax as an instance at 65 °C. During the solidification step, the suspensions are then poured into a rectangular shape of mould with their respective measurements and allows them to undergoes free crystalline at the room temperature. This step is to form solid composite samples and each respective samples takes about three hours of time range for complete solidification.

2.3. Material testing

2.3.1. Performing microscopic characterization (MC) analysis

2.3.1.1. Field Emission Scanning Electron Microscope (FESEM). The morphological structures of the mixed samples of MWCNTs and paraffin wax were examined using through the micrographs taken using the Field Emission Scanning Electron Microscope (FEI Quanta 400). Inspections of specimens were carried out by introducing a magnification of between 800 to 20,000x, with a distance of 1, 4 and 10 micrometre (—m). The equipment was operated at 20,000 kV on low vacuum. The obtained micrographs were used for discussions.

2.3.1.2. Thermogravimetric Analysis (TGA). To determine on the properties of the energy storage applications, melting and solidification temperature and their respective enthalpies of CNTs, a thermogravimetric analyzer (TGA) equipment will be used. TGA test consist of two different heating and cooling cycles which is in between the range of 10 and 80 °C with range of 5 °C each and also containing melting point of paraffin wax.

2.3.1.3. Fourier Transform Infrared Spectroscopy (FTIR). Characterization and evaluation on the structure surface of samples in terms of functional groups involved on the surface was examined by using the Perkin Elmer FT-IR Spectrometer Frontier model. The specimens were exposed to infrared radiation. The transmittance spectrum was observed in the region ranging of 4500 to 500 cm^{-1}. Meanwhile EDX is to investigate on chemical elements in each different mass fraction of CNTs and evaluate on the surface structure.

2.3.1.4. Mechanical testing.

2.3.1.4.1. Tensile testing Tensile testing was carried out on the specimens to determine the tensile properties of the mixture respective with the ratio of MWCNTs and paraffin wax following the ASTM D638-91 test method. The force required to break the sample specimen and the extent to which the specimen elongates to break point were measured. The mould used for this specimen is based on the Type 1 tensile bar dimension and thickness outlined by ASTM international, which was in a dog-bone shape mold. The tensile testing was conducted using LLYOD LR 10K Plus Advanced Universal Testing Machine (UTM), with cross-head speed of 10 mm/min. The testing was carried out by placing the specimens at a space allocated for the tester samples. The reading of the results can only be measured after the samples break into half to indicate the ending of the testing.

2.3.1.4.2. Flexural testing Flexural testing was carried out on the specimens to determine the bending strength of the composite materials for three-point loading condition, which indicates the materials stiffness, according to the ASTM D790 test method. The mold used for this specimen is based on the flexural bar dimension and thickness outlined by ASTM international. The flexural testing was conducted using LLYOD LR 10K Plus Advanced Universal Testing Machine (UTM), with cross-head speed of 1.5 mm/min. The testing was carried out by placing the specimens at a space allocated for the tester samples. The reading of the results can only be measured after the samples reach 5% fracture deflection point.

3. Results and discussion

3.1. Morphology of carbon nanofiller using FESEM

3.1.1. Dispersion of CNTs and paraffin wax

The microstructure and morphology of the pure paraffin wax and MWCNTs were examined by using the Field Emission Scanning Electron Microscope (FESEM). The surface properties of various mass percentage (Sample A, B, and C) were examined and studied through the SEM microstructure under three different magnifications of 1 μm, 4 μm and 10 μm as shown in Figs. 1–3.

Based on the figures illustrated in the lowest magnifications (1 μm), we can observe that there are significant changes on the structures of MWCNTs with the mixture of paraffin wax as the mass weight percentage increases. At first, the length of the nanotubes was difficult to determine as the size of aggregates was too small but it is manageable due to order of microns. For 1%-treated MWCNTs with paraffin wax (Sample A), it can be seen that there are less bundles of tangled tubes on its surfaces meanwhile 3% and 5% treated MWCNTs (Sample B and C) shows increase in bundles of tangled tubes. Sample C showed highest number of bundles of tangled tubes which agree to the hypothesis made earlier stating that 'the higher the mass weight percentage, the higher the number of tangled tubes observed (L. W. Fan et al. 2013). FESEM results showed that the treated MWCNTs together with paraffin wax initially have rough surface structures and in irregular shape. The roughness caused on the samples were due to the defect of paraffin wax on the surface of MWCNTs upon dispersing. Situations in such pores were detected and structural damage in the FESEM images of the samples were due to air were entrapped and rupture during processing the samples. When higher magnifications such as 10 μm were illustrated, the interphase between the two phases of MWCNTs and paraffin wax were observed more clearly.

Moreover, the sizes and distributions of CNTs upon dispersing into the paraffin wax has also been observed in Figs. 1–3. The sizes images has been proved that it is in the same agreement with the hypothesis made. The higher the mass weight percentage, from 1% to 5% with an increase of 2%, the higher the size and

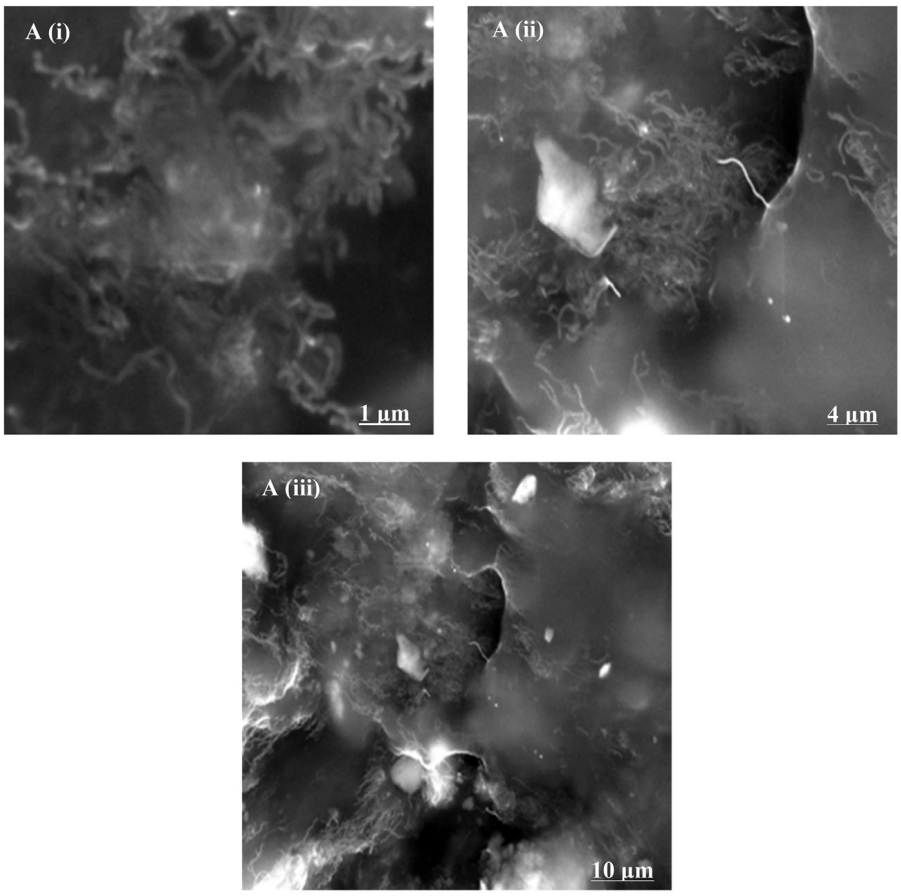

Fig. 1. SEM images of 1% dispersion of paraffin wax and MWCNTs with various scale: A (i) treated MWCNTs with 1 μm, A (ii) treated MWCNTs with 4 μm, A (iii) treated MWCNTs with 10 μm.

distribution of the samples. It is clearly clarify that CNTs has a wire-shaped nanofiller when it is well dispersed in the paraffin wax. During sample preparations, the MWCNTs are broken into smaller bunch due to the dispersion with paraffin wax. The 5% treated MCNTs has showed much bigger size differences than the 1% and 3% treated MCNTs.

Based on the purity trend of the samples, FESEM images at 1 μm, 4 μm and 10 μm for each mass weight percentage observed that the samples are free from impurities. This is because each samples were generated by using the optimum ratio of MWCNTs and paraffin wax by 1:1 which helps to generate chemical bonds on the surface walls, without giving any harms on the opening and closing ends of the MWCNTs. The same trend has been proven as shown in [1], that the lower dispersion of CNTs in the paraffin wax showed smaller number of tangled tubes rather than the higher percentage of dispersion which reveals that the correlations of weight percentage is parallel to the number of tangled tubes produced.

3.1.2. Transmission electron microscopic analysis

TEM analysis was conducted to determine the internal structure of the samples at optimum production condition with vary magnification scale as displayed in Fig. 4. The TEM images testified that the treated MWCNTs incorporated with paraffin wax at first have irregular shape and rough surface structure. This roughness affected on the samples were due to the paraffin wax defect on the MWCNTs surface upon dispersing. However at 200 nm magnification scale, the interphase between paraffin wax and MWCNTs two phases were observed more obviously.

3.2. Thermal conductivity properties

3.2.1. Dispersion of CNTs and paraffin wax

Furthermore, thermogravimetric (TGA) analysis were conducted for three different samples; 1% dispersion of paraffin wax and MWCNTs (Sample A), 3% dispersion of paraffin wax and MWCNTs (Sample B), as well as 5% dispersion of paraffin wax and MWCNTs (Sample C). Fig. 5 illustrated on the TGA curves with the comparison of three samples (Sample A, B, and C) corresponding to mass weight with respect to the temperature. As we know, thermal conductivity is an important analysis for phase change materials, since it gives an effect on the rate of energy storage and release. The thermal conductivity of PCM has been affected with the introduction of CNTs in the samples.

From the figure, it can be observed that thermal degradation occurs at lower temperature respective to mass weight loss of samples. The curves representing various temperatures are almost parallel to one another which indicated that temperature and mass weight have independent influences to each other. There were three different stages that can be identified during thermal conduction of organic phase change materials respective amount of dispersion with carbon nanotubes. Those stages can be classified as (i) evaporation of adsorbed water in the range 200–300 °C, (ii) primary pyrolysis method in the range of 300–400 °C with the release of gases and early development of basic structure of the samples ; and (iii) samples with dispersion of paraffin wax and CNTs are not volatile and thus remain as residues (Mubarak et al. 2014). The weight of Sample A decrease slightly with increasing temperature of 100 °C to 300 °C meanwhile Sample B decreases earlier than Sample A with increasing temperature

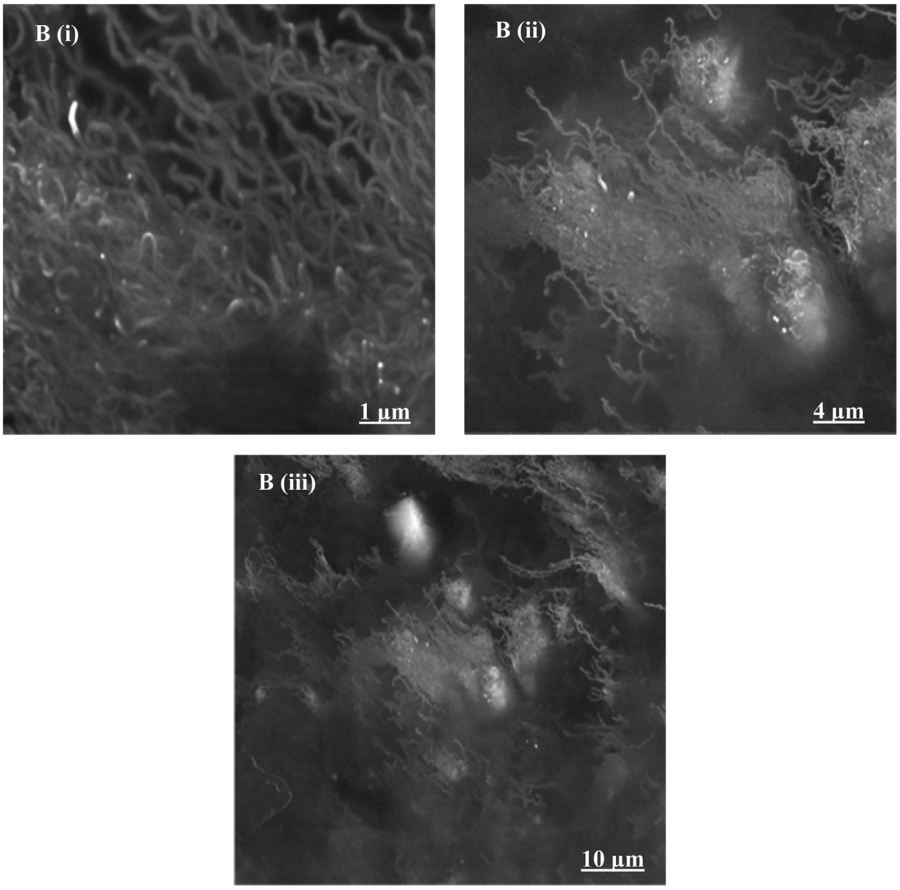

Fig. 2. SEM images of 3% dispersion of paraffin wax and MWCNTs with various scale: B (i) treated MWCNTs with 1 μm, B (ii) treated MWCNTs with 4 μm, B (iii) treated MWCNTs with 10 μm.

of 100 °C to 250 °C and Sample C decreases much earlier than Sample B and Sample A with increasing temperature from 100 °C to 220 °C. All three samples shows a decrement in weight loss due to water loss and uncertainty in structural stability with the release of increasing molecular weight compounds. With the increasing temperature of 300 °C to 400 °C, all three samples showed extreme depletion from weight of 90% to 5% due to MWCNTs undergoes oxidation process. At the final stage of temperature from 400 °C to 900 °C, the TGA curve for those three samples exhibit in constant profile respectively. These has proved that Sample A, B and C have inhibited to show a phase transitions since the materials had remained as residues since volatility does not occurs anymore after their inception temperature. The added CNTs that was dispersed into the paraffin wax has showed good and high thermal conductivity, which proves that it consists of high thermal conductivity network with their respective high length–width ratio.

Based on Fig. 5, the derivative peak of thermal degradation occurs for Sample A is at the higher temperature of 410 °C meanwhile Sample B is at temperature of 405 °C and Sample C at the lowest temperature of 400 °C. These illustrations proofed that each samples have its own index of higher thermal stability. In addition, the thermal conductive network becomes more compact with increasing in weight percentage of CNTs. This leads to further enhancing the thermal conductivity of Sample A, B and C based on their respective weight percentage.

Table 2
Chemical elements present in MWCNTs based on Sample A, B and C.

Elements	Chemical elements in MWCNTs samples in weight (%)		
	Sample A	Sample B	Sample C
C	88.65	90.85	97.66
O	8.42	7.39	1.19
Si	1.45	0.14	1.33
Al	0.75	–	0.36
Mg	0.35	–	–
Ca	0.37	–	–
Fe	–	–	0.07

3.3. Energy dispersive X-ray analysis

3.3.1. Dispersion of CNTs and paraffin wax

Energy dispersive X-ray (EDX) spectroscopy analysis were carried out in all three samples with their respective mass weight percentage of 1%, 3% and 5% on dispersion of paraffin wax and MWCNTs as Sample A, Sample B and Sample C. These analyses were carried out on determining the quantitative amount of different elements present in MWCNTs samples; such as carbon (C), oxide (O), silicon (Si), aluminium (Al), magnesium (Mg), calcium (Ca) and iron (Fe). The EDX results on amount of elements were plotted along with the respective sample A, B and C in Table 2.

Upon intermixing paraffin wax together with MWCNTs in a sample with parallel ratio of 1:1 with each other, amount of carbon content was compared based on the three samples. Based on the results obtained in Table 2, the lowest carbon content can be seen in Sample A and then increased with Sample B and finally Sample C. As observed, sample C showed highest amount of

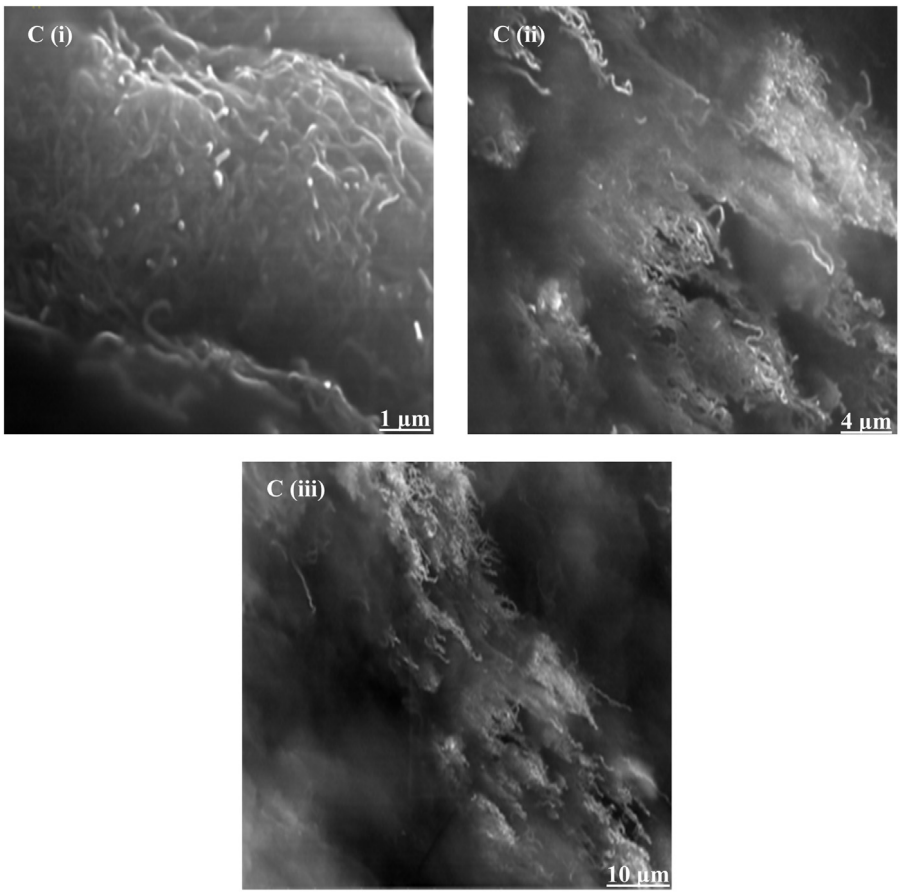

Fig. 3. SEM images of 5% dispersion of paraffin wax and MWCNTs with various scale: C (i) treated MWCNTs with 1 µm, C (ii) treated MWCNTs with 4 µm, C (iii) treated MWCNTs with 10 µm.

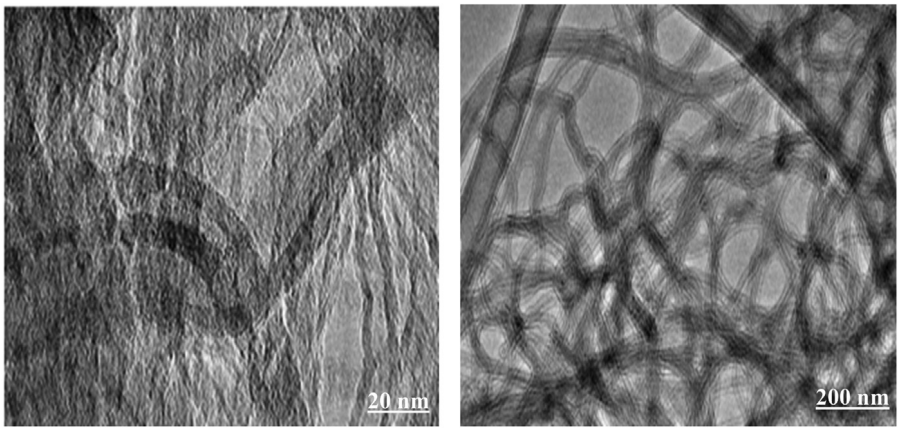

Fig. 4. High resolution transmission electron microscope analysis.

carbon content and lowest amount of oxide content. These is because when the samples were placed under the sonification bath treatment method, it generates more carbon functional group since additional reaction were prohibited. Moreover, it generates less oxide formation of oxidation process due to there were no involvement of any covalent bond in the samples. Based on the Table 2, it can be observed that there were no or less chemical elements such as Aluminium (Al), Magnesium (Mg), Calcium (Ca) and Iron (Fe) presents in Sample B and Sample C. These is due to the energy amount that has been deionized based on the carbon atom that has been present in this element [28].

Sample A, showed lowest carbon content is also due to the less amount of organic phase change materials that were intermixed together with MWCNTs. Therefore, it is proved that sonification bath method helped in obtaining higher carbon content based on amount of surface modifications of MWCNTs which were treated and exposed with paraffin wax. Fig. 6 illustrated on the EDX spectroscopy analysis of Sample C which verified on the presence of highest amount of carbon content. EDX results also indicated there were less detection and presence of other elements in Sample C after the sonification bath treatment method. Therefore, it can be concluded that samples undergoing sonification bath

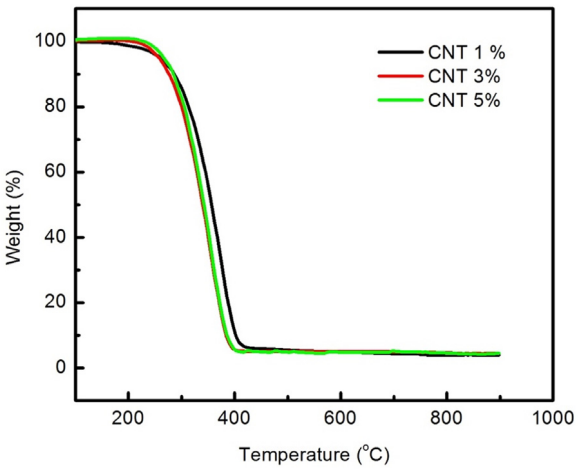

Fig. 5. TGA curves of Sample A, B and Sample C respective to various Weight and Temperature.

treatment without any addition reaction can produced higher carbon functional groups than any other methods.

3.4. Fourier Transform Infrared Spectroscopy (FTIR)

3.4.1. Dispersion of CNTs and paraffin wax

The Fourier Transform Infrared Spectroscopy (FTIR) were carried out on the samples and well-illustrated as shown in Fig. 7. Based on the figure plotted, it can be observed that absorption ranges in the spectrum for three samples (Sample A, Sample B and Sample C) from 400 cm^{-1} to 4000 cm^{-1}. The previous results showed that there were no detectable transmission band was observed with the pure paraffin wax with the same wavenumber range that is being covered in this study of properties. [29]

FTIR results based on Sample A, B and C shows a broad transmission band centred at almost 2913.97 cm^{-1} which gives a characteristics of hydrogen bonded –OH. Meanwhile, the band of the three samples showed a strong transmission band at around 720.45 cm^{-1} which can be clarified as bending stretch band of hydro –xyl groups and the band at 1462.81 cm^{-1} is proportional to the stretching bad of C–O. Finally, the transmission band at around 1084.86 cm^{-1} can be contributed to the stretching mode of –C=C– in an enol form.

Based on the results, it can be observed and indicated that –OH groups have been added to the surface structure of MWCNTs since there were small stretching of O–H band. These is because, there were only limited reactive efficiency takes place for oxide content in each samples based on the EDX results obtained earlier. Moreover, carbon atoms undergo oxidation process in the samples which that have initiated on the stretching band of C–O. Meanwhile, partial oxidation process during the purification process during manufacturing have made the presence of hydro –xyl groups on the surface of MWCNTs (Jun et al. 2018). The structure of treated MWCNTs backbone with different mass weight percentage were still preserved and kept even after sonification process has contributed to the stretching band of –C=C–.

3.5. Mechanical testing

3.5.1. Tensile properties

3.5.1.1. Young Modulus. Fig. 8 illustrates on the effect of organic phase change materials on tensile Young's Modulus of different mass percentage of carbon nanotubes (CNTs) obtained from the three-point flexural configuration as Sample 1 (1% dispersion of carbon nanotubes and paraffin wax), Sample 2 (3% dispersion of carbon nanotubes and paraffin wax), and Sample 3 (5% dispersion of carbon nanotubes and paraffin wax). The tensile Young's Modulus graph exhibits that it has an increasing linear trend for all composites with different mass percentage from 1 wt% to 3 wt% and then to 5 wt%. Based on the studies that has been carried out by [30], it clearly shows that tensile Young's Modulus studies of nanotechnology materials reinforced on organic phase change materials as the weight percentage increases. The studies conducted by respective author can be observed that the tensile modulus increases when the filler content increases in weight percentage. The main reason of the increment in these scenario is due to the stiffness of the reinforcement which gives an effect on the strength of the filler content. One of the reason on the increase from 1 to 3 wt% and then from 3 to 5 wt% of carbon nanotubes is due to the fact that as the filler increases, it causes more uniform distribution on the organic phase change materials, resulting an increase in the bonding between organic phase change materials and carbon nanotubes interphase. As we can observe in Fig. 7, it shows that Sample 2 shows less changes of tensile modulus compared to Sample 3. This can be the reason whereby agglomeration of the carbon nanotubes molecules around the organic phase change materials has caused an improper stability and curing of the dispersion. Another reason that contributes on these changes are might be due to increases in micropores between the carbon nanotubes and organic phase change materials that absorbs and weakened the adhesion surface between the carbon nanotubes and organic phase change materials. The Young's modulus of paraffin wax sheet at a large weight percentage converges perpendicular on the elastic modulus of MWCNTs. This can be observed more clearly since it increases as the weight percentage of CNTs increases. Greater distortion in C–C bonds in

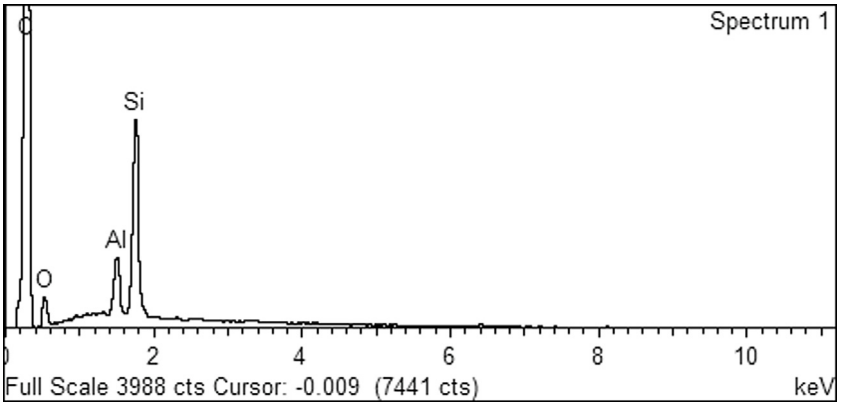

Fig. 6. EDX spectroscopy analysis of Sample C.

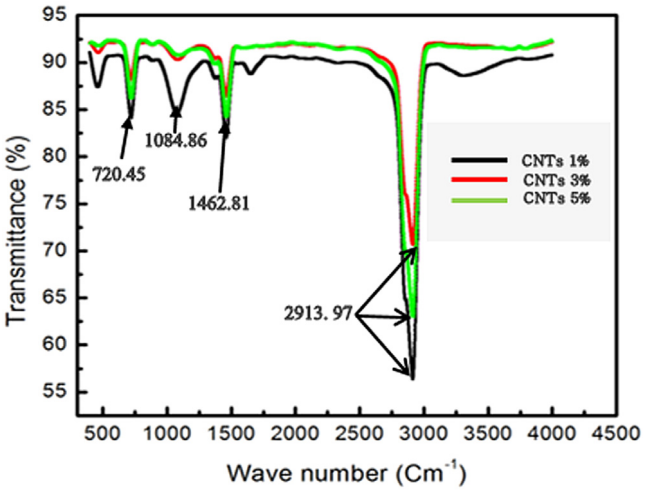

Fig. 7. FTIR spectrum of (a) Sample A (1% treated MWCNTs), (b) Sample B (3% treated MWCNTs) and (c) Sample C (5% treated MWCNTs).

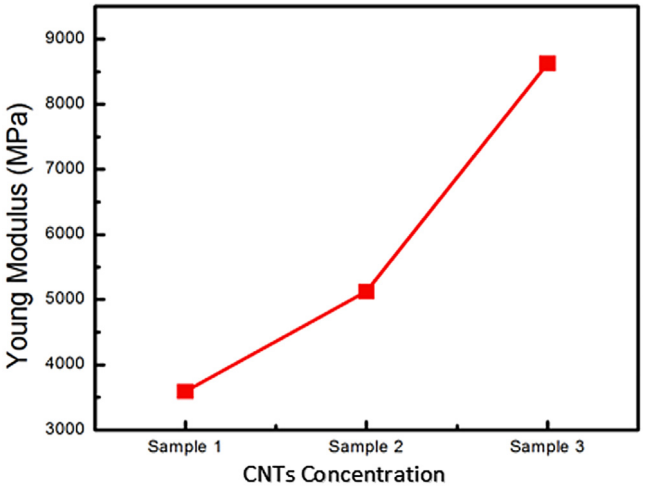

Fig. 8. Young's Modulus versus variation of weight percentage of CNTs.

larger weight percentage of CNTs have been produced compared to the smaller weight percentage. As shown in Fig. 8, the linear model showed clearly on the dependency of Young's modulus to CNTs weight percentage as it increases [31]. The results provided has been concluded with a good agreement between the trend of the results of this study and reported study of Rafii-Tabar (2004) who claimed that the values of Young's Modulus depend significantly on the thickness of the tube wall, whereby in this case, MWCNTs has been used.

3.5.1.2. Stress–strain elongation. Fig. 9 shows on the maximum bending stress obtained for three different samples with increasing weight percentage; Sample 1 (1 wt% dispersion of paraffin wax and carbon nanotubes), Sample 2 (3 wt% dispersion of paraffin wax and carbon nanotubes) and Sample 3 (5 wt% dispersion of paraffin wax and carbon nanotubes). Based on the graph obtained in Fig. 8, it can be observed that the maximum bending stress obtained at maximum load has decreases and inversely proportional compare to the graph obtained in Fig. 8 for Young's Modulus from 1 wt% to 5 wt% of filler contents. This is because percentage of stress elongation has been affected by the stiffness of the sample that initiates on the hypothesis whereby, the stiffer the sample preparation, the lower the percentage of stress elongation due

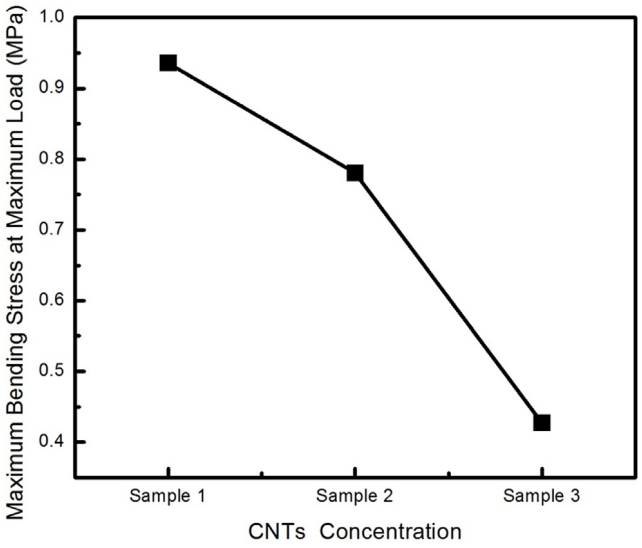

Fig. 9. Maximum Stress Elongation at various weight percentage of CNTs.

to different weight percentage. Moreover, formation of agglomeration within the increase of weight sample during mechanical testing has reduces the tensile elongation which then gives an effect on the formation of agglomeration. Agglomeration has always lead to lower adhesion between the surface of organic phase change materials and the filler reinforcement. In the study another study concluded that when the sample increases in weight percentage, the composite becomes heavier and tougher which then reduces the chain mobilization in the surface of paraffin wax as organic phase change materials [32]. The chain mobility decreases where there is a forming of cross-linked network in the chain, which prohibit high attractive forces to withstand on the surface of paraffin wax and carbon nanotubes. This has directly causes the brittleness of the composites to increases as the chain mobility decreases. Having brittleness on the composites have decreases on the tensile strength of the samples during the analysis being carried out. The reduction shown in the graph also explains on the higher frequencies that has been obtained during the sample preparation when it is reacted with paraffin wax has reflects on the cooling stresses generated by the contraction of paraffin wax [33].

Meanwhile, Fig. 10 shows the maximum bending strain that has been observed based the three same samples (Sample 1, Sample 2 and Sample 3) with respective filler content that has been used for stress elongation in Fig. 9 as above. The strain elongation has also showed the same trend of elongation which obtained in Fig. 9. It can be observed that as the filler content of carbon nanotubes increases, the strain elongation has an inversely proportional trend for 1 wt%, 3 wt% and 5 wt%. The elongation obtained for strain decreases with the increase in filler content which shows that despite in different weight percentage used for organic phase change materials, it can be observed that carbon nanotubes has similar trend since it act as reinforcing surface. Decrease in strain elongation has also reduces on the chain mobilization in the surface of organic phase change materials, which has discussed earlier in stress elongation and also due to the hardness of the sample during the sample preparation. The sample has contributed in higher effect of hardness due to the properties of carbon nanotubes on braking of two existing C–C bonds and the formation of two new C–C bonds. During this phase, multiple interfacial strain elongation takes place and this is accompanied by necking and breaking of carbon nanotubes in the samples [34].

Table 3
Comparison of various phase change materials using CNTs.

Adsorbent	SEM	TGA	EDX (Average percentage)	FTIR	Mechanical testing		References
					Tensile	Flexural	
Organic PCM with MWCNTs	Tangle of tubes increases at 1 μm, 4 μm and 10 μm for each different mass weight percentage of CNTs dispersion.	The peak of thermal degradation occurs for CNT 1% (Sample A), CNT 3% (Sample B) and CNT 5% (Sample C) is at various temperature between 400 °C to 410 °C.	–Carbon (92.39%) –Oxide (5.67%) –Silicon (0.97%) –Aluminium (0.56%) –Magnesium (0.35%) –Calcium (0.37%) –Iron (0.07%)	–OH (2913.97 cm^{-1}) –xyl (720.45 cm^{-1}) –C–O (1462.81 cm^{-1}) –C=C–(1084.86 cm^{-1})	CNT 1% (3500 MPa), CNT 3% (5100 MPa), CNT 5% (7800 MPa)	CNT 1% (25.5%), CNT 3% (26.25%), CNT 5% (28.0%)	This study
Organic PCM with phase changing epoxy blends	Paraffin particles shows an irregular shape and rough surface topography meanwhile epoxy metrics shows smooth profile	Degradation process occurs at 218 °C and neat paraffin at 209.4 °C.	–	–OH (3411cm^{-1}) –C–O (1095cm^{-1}) –xyl (782cm^{-1}) –C=C (1629cm^{-1})	53± 9 (Paraffin), 35 ± 4 (Epoxy)	2.00± 0.28 (Paraffin), 2.78± 0.19 (Epoxy)	[1]
MWCNTs and SWCNTs	Diameter of the SWCNTs and MWCNTs are approximately 20, 50 and 150 nm respectively.	CNT 1% (0.25 to 0.35 W/mK), CNT 3% (0.32 to 0.38 W/mK), CNT 5% (0.34 to 0.44 W/mK)	Temperature varies based on the process inhaled. At temperature range of 57 °C to 60 °C for melting process meanwhile 50 °C to 52 °C for solidification process		–	–	[8]

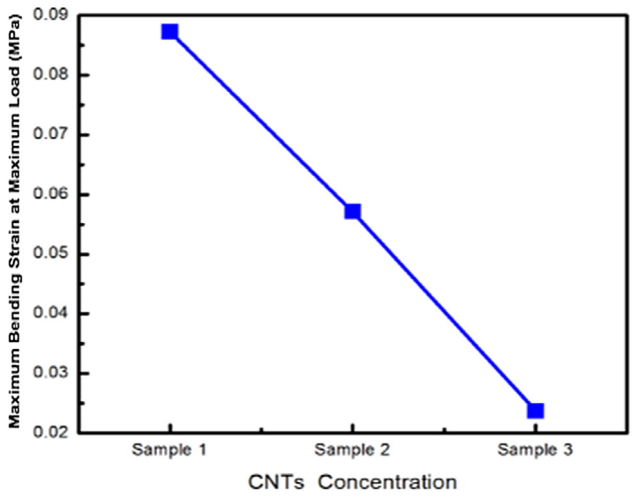

Fig. 10. Maximum Strain Elongation at various weight percentage of CNTs.

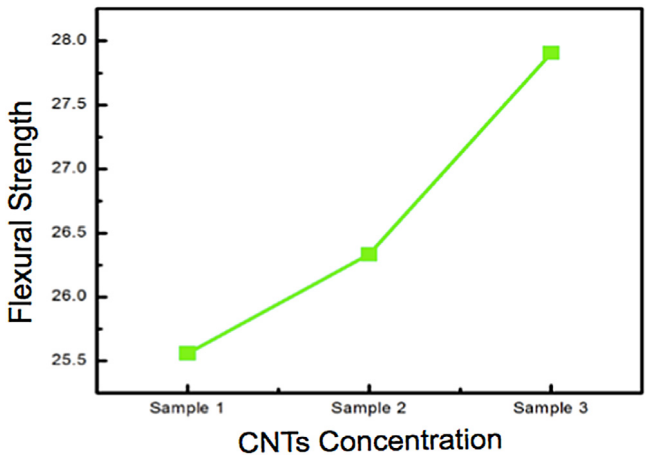

Fig. 11. Flexural Strength versus various weight percentage of CNTs.

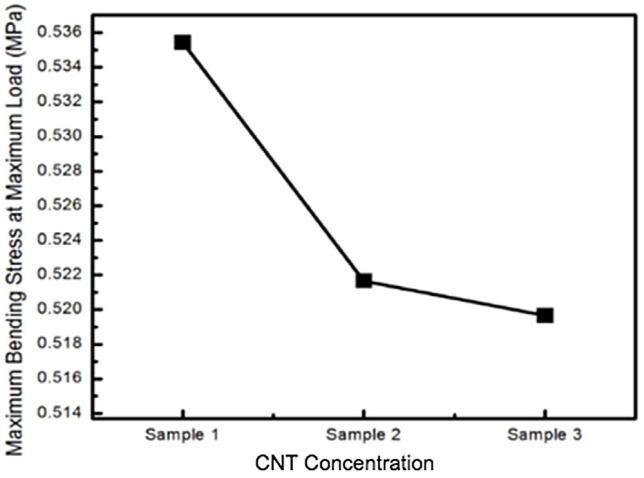

Fig. 12. Maximum Stress Elongation at various weight percentage of CNTs.

3.5.2. Flexural properties

3.5.2.1. Flexural strength. Flexural properties strength test was carried out on three various weight percentage samples that starts with Sample 1 (1 wt. % dispersion of paraffin wax and carbon nanotubes), Sample 2 (3 wt% dispersion of paraffin wax and carbon nanotubes) and Sample 3 (5 wt% dispersion of paraffin wax and carbon nanotubes) as shown in Fig. 11. The graph obtained shows that as the filler content increases, the flexural strength graph shows a linear increase for all composites from 1 wt% to 3 wt% and then increases with 5 wt%. The same scenario has been obtained in a study conducted by Deng et al. (2011), whereby the effect of different mass percentage of filler from 0 to 50% and has proved that the flexural strength increases as the mass percentage of filler content increases. As observed in Fig. 11, it can be observed that the reason of the increment in the flexural strength is due to strong interfacial bonding caused by the compatibility of the carbon nanotubes and surface of organic phase change materials. The higher the flexural strength, the higher the infusion due to good mixing of the reinforcing fillers towards the organic phase change materials. One of the reason on the trend of the graph obtained in Fig. 11 is also due to efficiency of the organic phase change materials that has strong interfacial adhesion to accept the presence of pores at the surface of the paraffin wax and the carbon nanotubes. The water absorption during these phase was very less, therefore it can be neglected and it directly contributes on higher wetting of the fibres in the samples.

3.5.2.2. Stress–strain elongation. Fig. 12 shows the effect of different weight percentage content on elongation percentage of fracture of paraffin wax with respective carbon nanotubes composite. The flexural elongation illustrates that as the filler content increases in the samples, the flexural elongation decreases for all composites sample 1, 2 and sample 3 with an increase of 2 wt% of each sample. As we can see, the sample 1 with 1 wt% of filler content shows that 53.543% fracture, meanwhile Sample 2 at 52.166% and finally at Sample 3 shows that 51.965% of fracture. This clearly illustrates that the reinforcing fillers decreases as the elongation percentage at fracture of the composites, which may be due to the reduction of polymer component inside the composites. As we know, the C–C bonds produced on the surface of carbon nanotubes and paraffin wax will initiates on higher stress than others upon breaking the first C–C bond. Upon the cleavage of two neighbouring C–C bonds in the composites, the size of the crack will become larger and contributes a reduction in critical stress scenario of MWCNTs will be initiated. Therefore, the C–C bonds nearby to those will break simultaneously [35]. As the weight percentage of carbon nanotubes increases, the size of the crack is large and that makes the elongation to break easily. This has been proven by adding higher filler content on other C–C bonds which has results in large crack.

Meanwhile Fig. 13, shows the same maximum bending strain that has been observed and discussed earlier in stress elongation of flexural properties. As the filler content increases in each samples, the strain elongation showed the same trend of elongation at which obtained in Fig. 12. The strain elongation graph illustrates that it has a reduction trend for 1 wt%, 3 wt% and 5 wt%. Critical strain has always known as the strain that corresponds to the maximum stress obtained. As shown in the graph, the loading of Sample 1 shows 6.325% fracture, meanwhile Sample 3 shows 3.595% and lastly Sample 3 shows 1.189% of strain elongation. The loading strain of Sample 1 made the C–C bond in the carbon nanotubes to stretch meanwhile when load of strain of Sample 3 increases, the C–C bonds stretched, break abruptly and brittle fracture was produced. Also, when load of strain Sample 5 increases much higher than Sample 1 and Sample 3, the stretching of C–C bonds increases and leads to higher brittle fracture on the surface of filler content and paraffin wax. The energy has been reduced and that contributes on reduction as the filler content increases because the strain energy is releasing [35].

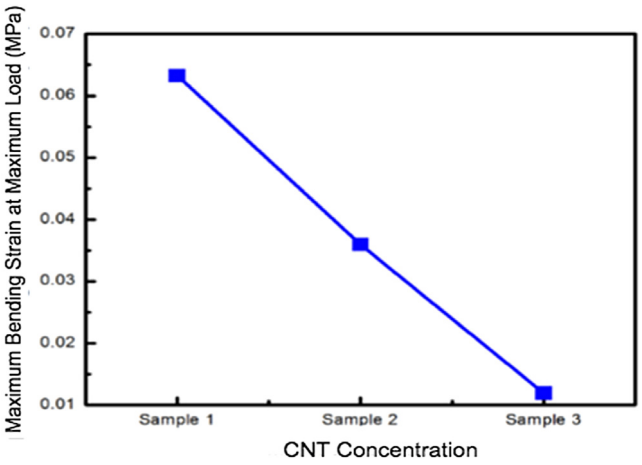

Fig. 13. Maximum Strain Elongation at various weight percentage of CNTs.

4. Conclusion

In conclusion, organic phase change materials have been always known for their best technology at recent years on fast developing nanotechnology field. Under the circumstances of organic phase change material, paraffin wax under the classification of paraffin is used to compare and identify on the best parameters via different analysis. The five analysis properties which have been carried out are morphology by using FESEM method, thermal conductivity, energy dispersion X-ray analysis, Fourier transform infrared spectroscopy and mechanical testing. From the research and literature review, the properties that has been identified were tested on the organic phase change materials together with the raw materials known as carbon nanotubes. These specifically covers on the multi-walled carbon nanotubes (MWCNTs), is because of their higher concentration carbon purity for more than 95% compare to the single-walled carbon nanotubes. Moreover, MWCNTs are a great filler to modify and improvise on various thermal and mechanical properties of organic phase change materials. The organic phase change materials and nanomaterials has been mixed in the ratio of 1:1. Overall results in the FESEM analysis has shown that the number of tangles increases as the weight percentage of the filler increases. The FESEM results also proved that carbon nanotubes consist of wire-shaped nanofillers when it is well dispersed in the paraffin wax. Meanwhile, thermal conductivity of CNTs in organic PCM shows a decrement in weight loss due to water loss and uncertainty in structural stability with the release of increasing molecular weight compounds. The energy dispersive X-ray analysis can be concluded that sample with higher weight percentage of fillers contributes on higher carbon content bond in the samples. The Fourier transform infrared spectroscopy analysis that been carried out proves that a broad transmission band centred at almost 2913.97 cm^{-1} which gives a characteristics of hydrogen bonded –OH. Meanwhile, the band of the three samples showed a strong transmission band at around 720.45 cm^{-1} which can be clarified as bending stretch band of hydro –xyl groups and the band at 1462.81 cm^{-1} is proportional to the stretching bad of C–O. Finally, the transmission band at around 1084.86 cm^{-1} can be contributed to the stretching mode of –C=C– in an enol form. Finally, mechanical testing analysis has enhanced the tensile and flexural strength and also Young's Modulus of paraffin wax respective to carbon nanotubes. The reduction obtained was observed in both tensile and flexural strength and modulus, which may be due to poor adhesion between surface interactions of carbon nanotubes as fillers and organic phase change materials. Based on the results obtained for each analysis, carbon nanotubes have proven and able to synthesis on the organic phase change materials. The experiments which was conducted has successfully fulfilled on the aims and objectives of this thesis by proving carbon nanotubes has showed important facts on synthesizing organic phase change materials. The excellent chemical compatibility, thermal stability and durability upon dispersing CNTs with organic PCMs have enlighten and benefits for thermal energy storage applications such as building energy conservation and domestic hot water and heating systems. These promising results has showed that CNTs enhance and gives a great potential on organic phase change materials in the nanotechnology industry.

Declaration of competing interest

Authors Declare that no conflict of interest.

References

[1] G. Fredi, A. Dorigato, L. Fambri, A. Pegoretti, Wax confinement with carbon nanotubes for phase changing epoxy blends, Polymers 9 (9) (2017) 405.
[2] Z. Ling, J. Chen, T. Xu, X. Fang, X. Gao, Z. Zhang, Thermal conductivity of an organic phase change material/expanded graphite composite across the phase change temperature range and a novel thermal conductivity model, Energy Convers. Manage. 102 (2015) 202–208.
[3] N. Sahan, H.O. Paksoy, Thermal enhancement of paraffin as a phase change material with nanomagnetite, Sol. Energy Mater. Sol. Cells 126 (2014) 56–61.
[4] S. Lavinia Gabriela, Thermal energy storage with phase change material, Leonardo Electron. J. Pract. Technol. 11 (20) (2012) 75–98.
[5] J. Wang, H. Xie, Z. Xin, Y. Li, L. Chen, Enhancing thermal conductivity of palmitic acid based phase change materials with carbon nanotubes as fillers, Sol. Energy 84 (2) (2010) 339–344.
[6] T.A.O. Zheng, J.R. Dahn, CHAPTER 11 - applications of carbon in Lithium-Ion batteries, in: T.D. Burchell (Ed.), Carbon Materials for Advanced Technologies, Elsevier Science Ltd, Oxford, 1999, pp. 341–387.
[7] N. Sarier, E. Onder, Organic phase change materials and their textile applications: An overview, Thermochim. Acta 540 (2012) 7–60.
[8] L.-W. Fan, X. Fang, X. Wang, Y. Zeng, Y.-Q. Xiao, Z.-T. Yu, X. Xu, Y.-C. Hu, K.-F. Cen, Effects of various carbon nanofillers on the thermal conductivity and energy storage properties of paraffin-based nanocomposite phase change materials, Appl. Energy 110 (2013) 163–172.
[9] T. Li, J.-H. Lee, R. Wang, Y.T. Kang, Heat transfer characteristics of phase change nanocomposite materials for thermal energy storage application, Int. J. Heat Mass Transfer 75 (2014) 1–11.
[10] H. Zhang, Q. Sun, Y. Yuan, Z. Zhang, X. Cao, A novel form-stable phase change composite with excellent thermal and electrical conductivities, Chem. Eng. J. 336 (2018) 342–351.
[11] A. Aqel, K.M.M.A. El-Nour, R.A.A. Ammar, A. Al-Warthan, Carbon nanotubes, science and technology part (I) structure, synthesis and characterisation, Arab. J. Chem. 5 (1) (2012) 1–23.
[12] Z. Han, A. Fina, Thermal conductivity of carbon nanotubes and their polymer nanocomposites: A review, Prog. Polym. Sci. 36 (7) (2011) 914–944.
[13] J.Y. Lim, N.M. Mubarak, M. Khalid, E.C. Abdullah, N. Arshid, Novel fabrication of functionalized graphene oxide via magnetite and 1-butyl-3-methylimidazolium tetrafluoroborate, Nano-Struct. Nano-Objects 16 (2018) 403–411.
[14] M.J. Yee, N.M. Mubarak, M. Khalid, E.C. Abdullah, P. Jagadish, Synthesis of polyvinyl alcohol (PVA) infiltrated MWCNTs buckypaper for strain sensing application, Sci. Rep. 8 (1) (2018) 17295.
[15] S. Yuan, S. Chen, Z. Hu, G. Jiang, Y. Zhang, Y. Yang, P. Xiong, X. Zhu, J. Xiong, Reduced graphene oxide and carbon/elongated TiO2 nanotubes composites as anodes for Li-ion batteries, Nano-Struct. Nano-Objects 12 (2017) 27–32.
[16] C. Kumar, A. Gaur, S.K. Rai, P. Maiti, Piezo devices using poly(vinylidene fluoride)/reduced graphene oxide hybrid for energy harvesting, Nano-Struct. Nano-Objects 12 (2017) 174–181.
[17] W. Khan, A.K. Singh, S. Naseem, S. Husain, M. Shoeb, M. Nadeem, Synthesis and magnetic dispersibility of magnetite decorated reduced graphene oxide, Nano-Struct. Nano-Objects 16 (2018) 180–184.
[18] M.M. Rahman, M.A. Hussein, K.A. Alamry, F.M. Al-Shehry, A.M. Asiri, Polyaniline/graphene/carbon nanotubes nanocomposites for sensing environmentally hazardous 4-aminophenol, Nano-Struct. Nano-Objects 15 (2018) 63–74.
[19] S.R. Anjum, V.N. Narwade, K.A. Bogle, R.S. Khairnar, Graphite doped hydroxyapatite nanoceramic: Selective alcohol sensor, Nano-Struct. Nano-Objects 14 (2018) 98–105.

[20] A. Karmakar, T. Mallick, S. Das, N.A. Begum, Naturally occurring green multifunctional agents: Exploration of their roles in the world of graphene and related systems, Nano-Struct. Nano-Objects 13 (2018) 1–20.
[21] M. Sharma, S. Ramakrishnan, S. Remanan, G. Madras, S. Bose, Nano tin ferrous oxide decorated graphene oxide sheets for efficient arsenic (III) removal, Nano-Struct. Nano-Objects 13 (2018) 82–92.
[22] H. R, J. M, P. Haridoss, C.P. Sharma, Novel nano-cocoon like structures of polyethylene glycol–multiwalled carbon nanotubes for biomedical applications, Nano-Struct. Nano-Objects 13 (2018) 30–35.
[23] W. Clower, N. Groden, C.G. Wilson, Graphene nanoscrolls fabricated by ultrasonication of electrochemically exfoliated graphene, Nano-Struct. Nano-Objects 12 (2017) 77–83.
[24] K. Sagara, Latent heat storage materials and systems: A review AU - Sharma, S.D, Int. J. Green Energy 2 (1) (2005) 1–56.
[25] C. Alkan, K. Kaya, A. Sarı, Preparation, thermal properties and thermal reliability of form-stable paraffin/polypropylene composite for thermal energy storage, J. Polymers Environ. 17 (4) (2009) 254.
[26] F.S.A. Khan, N.M. Mubarak, M. Khalid, E.C. Abdullah, Functionalized Carbon nanomaterial for artificial bone replacement as filler material, in: S. Inamuddin, R. Thomas, Kumar Mishra, A.M. Asiri (Eds.), Sustainable Polymer Composites and Nanocomposites, Springer International Publishing, Cham, 2019, pp. 783–804.
[27] N.M. Mubarak, J.N. Sahu, E.C. Abdullah, N.S. Jayakumar, P. Ganesan, Single stage production of carbon nanotubes using microwave technology, Diam. Relat. Mater. 48 (2014) 52–59.
[28] L.Y. Jun, N.M. Mubarak, L.S. Yon, C.H. Bing, M. Khalid, E.C. Abdullah, Comparative study of acid functionalization of carbon nanotube via ultrasonic and reflux mechanism, J. Environ. Chem. Eng. 6 (5) (2018) 5889–5896.
[29] H. Pan, L. Liu, Z.-X. Guo, L. Dai, F. Zhang, D. Zhu, R. Czerw, D.L. Carroll, Carbon nanotubols from mechanochemical reaction, Nano Lett. 3 (1) (2003) 29–32.
[30] H. Zhong, J.R. Lukes, Interfacial thermal resistance between carbon nanotubes: Molecular dynamics simulations and analytical thermal modeling, Phys. Rev. B 74 (12) (2006) 125403.
[31] R. Rafiee, M. Heidarhaei, Investigation of chirality and diameter effects on the young's modulus of carbon nanotubes using non-linear potentials, Compos. Struct. 94 (8) (2012) 2460–2464.
[32] L. Deng, S.J. Eichhorn, C.-C. Kao, R.J. Young, The effective Young's Modulus of carbon nanotubes in composites, ACS Appl. Mater. Interf. 3 (2) (2011) 433–440.
[33] O. Lourie, H.D. Wagner, Evaluation of Young's Modulus of carbon nanotubes by micro-Raman spectroscopy, J. Mater. Res. 13 (9) (2011) 2418–2422.
[34] C. Wei, K. Cho, D. Srivastava, Tensile strength of carbon nanotubes under realistic temperature and strain rate, Phys. Rev. B 67 (11) (2003) 115407.
[35] Q. Yuan, L. Li, Q. Li, F. Ding, Effect of metal impurities on the tensile strength of carbon nanotubes: A theoretical study, J. Phys. Chem. C 117 (10) (2013) 5470–5474.